International Journal of Heat and Fluid Flow 63 (2017) 139–148

Contents lists available at ScienceDirect

International Journal of Heat and Fluid Flow

journal homepage: www.elsevier.com/locate/ijhff

On coherent structures and mixing characteristics in the near field of a rotating-pipe jet

R. Mullyadzhanov[a,b,*], S. Abdurakipov[a,b], K. Hanjalić[b,c]

[a] Institute of Thermophysics SB RAS, Lavrentyeva 1, Novosibirsk 630090, Russia
[b] Novosibirsk State University, Pirogova 2, Novosibirsk 630090, Russia
[c] Delft University of Technology, ChemE Dept., Julianalaan 136, 2628 BL Delft, The Netherlands

ARTICLE INFO

Article history:
Available online 26 July 2016

Keywords:
Swirling jets
Mixing
Coherent structures

ABSTRACT

Mixing characteristics and coherent structures populating the near-nozzle area of a rotating-pipe jet at the Reynolds number of 5300 were studied by Large-eddy simulation (LES). The swirl rate, defined as the ratio of the tangential velocity of the inner pipe wall to the bulk axial velocity, varied from 0 to 1, corresponding to a weak-to-moderate swirl intensity, insufficient to induce reverse flow near the nozzle. The visualization shows that for the non-swirling jet the near-wall streaky structures generated in the pipe interact with the shear layer, evolving into hairpin-like structures that become tilted at low rotation rates. For higher swirl, they cannot be recognized as they are destroyed at the nozzle exit. No large-scale coherent structures akin to Kelvin–Helmholtz vortical rings in the 'top-hat' jets are identifiable close to the nozzle. Using the single and joint probability density functions of velocity and passive scalar (temperature) fields we quantify the events responsible for the intensive entrainment at various swirl numbers. The isosurface of the temperature field indicates the meandering and precessing motion of the rotating jet core at the axial distance of 6*D* downstream, where *D* is the diameter of the pipe. The Fourier analysis with respect to the azimuthal angle and time reveals an interplay between the co- and counter-rotating modes. These findings explain the previously detected but not fully clarified phenomenon of the weakly counter-rotating jet core at low swirl rates.

1. Introduction

Swirling flows have long been in the research focus because of their versatile industrial application for promoting mixing, phase separation, flame stabilization and control, but also because of their interesting flow physics. Among the variety of configurations, the free swirling jets have a kind of canonical significance as they contain most generic features of swirling flows, but are void from the effects of confinement and solid walls. The rotation-generated pressure gradient that dominates the jet near-field at strong swirl rates with a consequent vortex breakdown and flow recirculation, and enhanced mixing and entrainment of surrounding fluid imparted by the swirl-induced shear, are the main features that distinguish the swirling jets from their non-swirling surrogate.

A round jet is usually generated by forcing fluid through a smooth-contraction nozzle generating a close-to-laminar 'top-hat' velocity profile (Ball et al., 2012). However, it is well known that the nozzle shape and geometry as well as the upstream conditions determine the characteristics of the jet through the level of turbulence and the momentum thickness of the boundary layer at the nozzle walls. Moreover, the nozzle with a contraction produces an undesired overshoot at the centre of the axial velocity profile when a moderate level of rotation is applied to the flow inside the swirl-generating device (Alekseenko et al., 2008; Billant et al., 1998; Leclaire and Jacquin, 2012; Oljaca et al., 1998; Panda and McLaughlin, 1994). Thus, in order to analyze possible flow regimes one needs to vary a wide range of parameters. Inevitably, issues arise when the results are compared with those obtained by other researchers using different swirling facilities. A reliable and comprehensive data-set on a well-defined canonized swirling jet is thus much desired to serve as a reference for benchmarking other numerical and experimental studies on swirling flows.

When considering a canonical jet, one tries to reduce the number of dimensionless parameters governing the flow. To eliminate the effects of nozzle geometry, a plausible option is to study the jet issuing from a round pipe. If the pipe is long enough, the flow at the exit corresponds to the fully developed turbulent regime where only one parameter, i.e., the Reynolds number, determines the flow.

* Corresponding author.
E-mail address: rustammul@gmail.com (R. Mullyadzhanov).

http://dx.doi.org/10.1016/j.ijheatfluidflow.2016.06.018
0142-727X/

In case of swirling flows, a long pipe rotating around its axis represents a canonical swirling jet with a unique inflow velocity profile unlike various swirling devices (Örlü, 2009). In the present work with the use of Large-eddy simulations (LES) we focus on the rotating pipe jet at low-to-moderate swirl. The inflow conditions are provided with a separate periodic pipe flow simulations mimicking very long supplying duct. The Reynolds number, Re, based on the bulk velocity U_b and pipe diameter D, is 5300 and swirl number $N = U_w/U_b$ varies from 0 to 1, where U_w is the tangential velocity of the pipe rotating around its axis.

One of the first experiments on a rotating pipe jet was performed by Rose (1962). He described the bulk effect of swirl such as the increase of the spreading and entrainment rates together with the higher level of turbulence and faster decay of the axial velocity compared to the non-rotating jet. Pratte and Keffer (1972) confirmed conclusions of Rose and examined the streamwise variation of the mean axial and tangential velocity showing x^{-1} and x^{-2} dependence, respectively, where x is the streamwise coordinate, which is in agreement with the theoretical considerations by Loitsianskii (1953), Mullyadzhanov and Yavorskii (2013), among others. Mehta et al. (1991) quantified the changes in the Reynolds stresses with the increase in N up to 0.4. Facciolo and Alfredsson (2004) studied a swirling pipe jet at Re up to 33,500 and $N = 0.5$. The experimental facility featured a long enough pipe of $100D$ to provide a fully developed turbulent conditions at the nozzle exit. They studied the near-field time-averaged turbulent characteristics and observed the phenomenon of the weak jet core counter-rotation around $x = 6D$ attributing it to the effect of the Reynolds stresses on the mean field. Further experimental and numerical observations are described by Facciolo et al. (2007) focusing on both, the rotating pipe and jet flows. Örlü and Alfredsson (2008) used the same setup to perform simultaneous velocity and passive scalar point measurements of a slightly heated swirling air pipe jet at $Re = 24,000$ and $N = 0.5$ together with a non-swirling counterpart. They observed high intermittency of both fields and calculated joint probability density distributions of velocity components and temperature. Maciel et al. (2008) using LES and experimental data discussed the phenomenon of counter-rotating core and proposed an explanation in terms of the angular momentum transport.

A swirling quasi-laminar flow issuing from a relatively short pipe has been investigated experimentally by Liang and Maxworthy (2005) at $Re = 1000$. The authors studied the flow at different rotation rates observing various azimuthal instabilities in the form of helical waves at moderate swirl numbers. Particular attention has been paid to the global instability mode as a result of the vortex breakdown regime with reverse flow region near the nozzle at high rotation rates causing large-scale fluctuations in the form of a spiral vortex. The vortex breakdown phenomenon attracted a lot of attention in the literature and is well reviewed by Lucca-Negro and O'Doherty (2001) among others. Using LES Luginsland and Kleiser (2015), Luginsland (2015) and Luginsland et al. (2016) studied the laminar inflow pipe jet with solid-body rotation and $N \approx 1.3$ featuring reverse flow near the pipe exit. They observed high sensitivity of the position and size of the vortex breakdown bubble to boundary conditions, thickness of the pipe wall and inflow perturbations. Sanmiguel-Rojas et al. (2008) investigated numerically the laminar flow discharging from a rotating pipe into a cylindrical container through a 1: 8 sudden expansion. They showed a transition map for various flow regimes in the $Re - N$ plane, analyzed helical perturbations generated in the rotating pipe and their effect on the jet flow and vortex breakdown phenomenon. Recently Miranda-Barea et al. (2015) performed experiments confirming the results of Sanmiguel-Rojas et al.

The paper is organized as follows. Section 2 describes the computational details and flow configuration. In Section 3 we describe the time-averaged characteristics of the flow. The dynamical features are analyzed in Section 4 followed by conclusions.

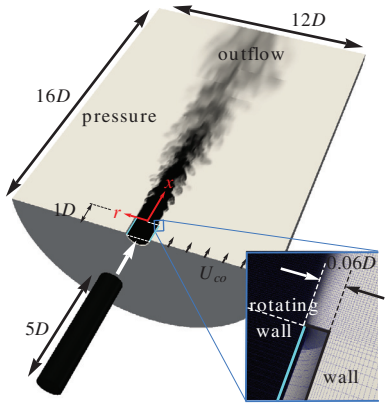

Fig. 1. Half of the computational domain, cylindrical coordinate system (r, ϕ, x) and boundary conditions. The instantaneous field is visualized by the temperature. The $5D$ pipe is used to simulate the unsteady inflow conditions with a periodic boundary conditions.

2. Governing equations and computational details

The LES is performed with the TU Delft unstructured finite-volume computational code T-FlowS (Ničeno and Hanjalić, 2005). The diffusion and convection terms are discretised by the second-order central-difference scheme, whereas the time-marching is performed using a fully-implicit three-level time scheme. We solve the non-dimensional spatially filtered transport equations for mass, momentum and passive scalar (temperature) to determine the dynamics and mixing of the incompressible fluid:

$$\frac{\partial U_i}{\partial x_i} = 0,$$
$$\frac{\partial U_i}{\partial t} + \frac{\partial U_i U_j}{\partial x_j} = -\frac{\partial P}{\partial x_i} + \frac{1}{Re}\frac{\partial^2 U_i}{\partial x_j^2} - \frac{\partial \tau_{ij}}{\partial x_j},$$
$$\frac{\partial T}{\partial t} + \frac{\partial T U_j}{\partial x_j} = \frac{1}{PrRe}\frac{\partial^2 T}{\partial x_j^2} - \frac{\partial q_j}{\partial x_j},$$

where U_i and T are the resolved velocity vector and temperature. We assume the working fluid to be air with the Prandtl number, $Pr = \nu/\alpha = 0.71$, where ν is the kinematic viscosity of the fluid and α its thermal diffusivity. The stress tensor τ_{ij} represents the influence of the subgrid scales on resolved motion and is modelled using the dynamic Smagorinsky model as follows, $\tau_{ij} = -2\nu_t S_{ij} + \tau_{kk}\delta_{ij}/3$, where S_{ij} is the strain-rate tensor, δ_{ij} the Kronecker delta and $\nu_t = (C_s\Delta)^2\sqrt{2S_{ij}S_{ij}}$ the turbulent viscosity. The Smagorinsky constant C_s is determined dynamically according to the standard routine (Germano et al., 1991); Δ is the local grid size. The subgrid-scales heat flux term is defined in a similar manner, $q_j = (\nu_t/Pr_t)(\partial T/\partial x_j)$, where the turbulent Prandtl number is assumed constant, $Pr_t = 0.9$.

We consider a fully turbulent canonical rotating-pipe jet configuration. The computational domain was in the form of a cylinder of $12D$ in diameter and $16D$ in length, Fig. 1. A precursor simulation of the fully developed $5D$-long rotating pipe flow generated the inflow conditions for each N considered (see Appendix A). A stored time series of the precursor unsteady velocity field was then imposed as the inflow conditions at the $r - \phi$ cross-section at the inlet ($x = -1D$) of a $1D$-long pipe segment immersed into the computational domain, Fig. 2. The incoming flow with $Re = 5300$ and N varying from 0 to 1 with a step of 0.25 had a normalized temperature $T = 1$. A small co-flow of $U_{co} = 0.04U_b$ with $T = 0$ was